

ARTICLE

Open Access



Particle size of ginseng (*Panax ginseng* Meyer) insoluble dietary fiber and its effect on physicochemical properties and antioxidant activities

Guihun Jiang^{1†}, Zhaogen Wu^{1†}, Kashif Ameer³, Shanji Li^{1*} and Karna Ramachandraiah^{2*}

Abstract

Dietary fibers (DFs) and associated phytochemicals in ginseng species are known to provide various functional and health benefits. The incorporation of ginseng insoluble dietary fiber (IDF) in food products often result in undesirable physicochemical properties. Thus, to overcome such demerits, micronization of IDF has been considered. This study investigated the effect of particle size on the physicochemical properties, antioxidant activities, structure and thermal analysis of ginseng IDF. Micronized IDF powder with median particle diameter of 15.83 μm was produced through fine grinding. Reduction of ginseng IDF resulted in increased brightness, water holding capacity and solubility. Decreasing particle sizes also lowered bulk, tapped density, Carr index and Hausner ratio. Reduction of particle size caused greater extractability of mineral and phenolic content and thereby increasing the DPPH radical scavenging activity and ferric reducing antioxidant power. Increased polyphenol extraction with smaller particle size also lowered the mice erythrocytes hemolysis percentage while the hemolysis inhibition rate was increased. Particle size also influenced the thermal stability of ginseng IDF powders. FTIR spectra revealed lack of impact on the major phenolic structures due to superfine grinding. Hence, micronized ginseng IDF powders with improved physicochemical properties and antioxidant activities possess the potential to be used in food and pharmaceutical industries.

Keywords: Ginseng, Insoluble dietary fiber, Superfine grinding, Physicochemical properties, Antioxidant activities

Introduction

Several studies have elucidated various functional and health benefits of dietary fibers (DFs) including reducing postprandial glycemic index while maintaining gastrointestinal function and lowering the risk of cardiovascular diseases, diabetes and colon cancer [1]. The other functional effects of DFs include influences on water holding capacity (WHC) and oil holding capacity (OHC), which could be potentially utilized in the development or

reformulation of food products. DFs are defined as carbohydrate polymers primarily derived from the cell walls of plants with two or more monomeric units [2]. DFs can be directly obtained from natural sources such as cereals, vegetables, and fruits. For the enrichment of foods, fibers with particular properties have been extracted, isolated and modified from various sources. Fibers are derived mainly from natural raw materials via chemical, physical and enzymatic methods [3]. DFs are classified based on some parameters that include major source, chemical structure and water solubility [4].

DFs are usually non-starch polysaccharides that possess the ability to withstand digestion and absorption in the small intestine, undergoing full or partial fermentation in the large intestine of humans [4]. DFs are also

*Correspondence: shanji@hotmail.com; karna@sejong.ac.kr

[†]Guihun Jiang and Zhaogen Wu contributed equally to this work

¹ School of Public Health, Jilin Medical University, Jilin 132013, China

² Department of Food Science and Biotechnology, Sejong University, Seoul 05006, South Korea

Full list of author information is available at the end of the article

classified based on water solubility as water soluble DFs (pectin and some hemicelluloses) and water in-soluble DFs (cellulose or lignin). It is the insoluble dietary fibers (IDF) that regulate the intestinal function via improving the intestinal peristalsis and fecal volume and removing heavy metals, grease, and other unwanted substances [2, 5]. To achieve best activity of DFs, about 50–75% of IDF in daily meals is recommended [4]. Furthermore, soluble DF (SDF), which are higher in fruits and vegetables than cereals, are also required along with IDF. DFs can also act as prebiotics, which function as sources of carbon for the growth of gastrointestinal microbiota. Inulin, galactooligosaccharides and fructooligosaccharides, are the well-known prebiotics [6]. However, it is important to note that the functional benefits of DFs are contingent upon the structural and chemical composition of DFs [4].

Panax ginseng Meyer, which usually refers to the root of the *Panax* genus, has long been widely used as a curative agent in Eastern Asia, North America, and Europe [7]. The utilization of ginseng root is more favored due to the presence of pesticide residue in other parts such as leaf or stem [8]. Ginseng has been shown to exhibit immunomodulatory properties that promote a wide range of antimicrobial functions. However, immunomodulatory properties are highly affected by factors such as type and source of ginseng, and extraction method [9]. The variation in such properties is attributed to the various phytochemicals that include ginsenosides, carbohydrates, phytosterols, polyacetylenes, polyphenolic compounds, sugars, acidic polysaccharides, organic acids, amino acids, vitamins, nitrogenous substances, and minerals. In particular, ginsenosides are known to provide various health benefits that include antioxidant, anti-inflammatory and immunity enhancing activities. Owing to the aforementioned bioactive agents along with dietary fibers, ginseng is used as nutritional supplement, herbal remedy [10] and adjuvants during vaccination [11]. However, acceptability of DFs in final product is dependent upon the interaction of DFs with components and ingredients utilized [4]. In particular, IDF has been shown to negatively impact the color, texture and flavor of the final product. To overcome such demerits, DFs have been modified using sulfuric acid (low concentration) and blasting extrusion. However, the most effective method was found to be with enzymatic treatment [12].

Micronization involves the reduction of average particle size of raw materials [13]. Particle size reduction of raw materials has been shown to modify structural characteristics and improve technological properties [14]. Particle size is known to influence physico-chemical properties such as water-holding capacity, solubility and flowability. However, a major constraint in production of superfine powders is the nature of raw materials.

Particularly, hardness and rough texture of materials can influence the average particle size of its powders [13]. Furthermore, health benefits derived from ginseng are dependent on dietary fibers, making it necessary to evaluate the impact micronization on ginseng IDF. In addition, functional properties, such as adsorption to cholesterol and oil, are mostly due to IDF than SDF [5]. As a result, micronization of IDF has gained increased attention [15]. Since studies pertaining to micronization of ginseng IDF are limited, this study focused on the structural characteristics and technological functionalities of micronized ginseng IDF. This study systematically analyzes composition, structure, physicochemical, and technological properties of IDF as influenced by micronization.

Materials and methods

Materials

Dried ginseng roots were purchased from a local supermarket in Jilin city (longitude 125° 40' ~ 127° 56', latitude 42° 31' ~ 44° 40'), China. The ginseng roots cultivated for 5 years were collected in November 2019. All chemicals and reagents used in this study were of analytical grade. Trichloroacetic acid, hydrogen peroxide, ferric chloride, potassium ferricyanide, sodium carbonate, methanol were supplied by Zhengda Chemical Company, Jilin, China. α -amylase, amyloglucosidase, protease, gallic acid, 1,1-Diphenyl-2-picrylhydrazyl were obtained from Sigma-Aldrich (St. Louis, MO, USA).

Preparation of ginseng residue

Ginseng residue was prepared according to Hua et al. [5]. Briefly, Ginseng residue was formed after ginseng polysaccharides were extracted by boiling. The residue was then washed with ethanol and distilled water for the removal of water-soluble oligosaccharide and inorganic salts. The residue was dried (60 °C for 24 h), sieved (60 mesh), packaged in a self-sealing bag, and stored at – 20 °C until further analysis.

Extraction of ginseng IDF

The obtained ginseng residue was then used for the preparation of the IDF as described by Bunzel et al. [16] with some modification. Ginseng residue (60 g) was treated with 1.8 mL heat-stable α -amylase in 1.5 L of buffer (pH 6.0) using a water bath at 95 °C for 20 min. The pH of reactants was adjusted to 7.5, protease (3.0 mL) was added at 60 °C and incubated for 1 h. Later, amyloglucosidase (1.2 mL) was added to the reaction mixture with pH adjusted to 4.5 at 60 °C for the removal of starches and proteins. Finally, the reaction mixture was centrifuged at 5000 rpm for 20 min, and the residue was then washed twice with distilled water and 95% ethanol. Precipitate was dried at 50 °C for 24 h to yield IDF. The ginseng IDF

was then packaged in an aluminum-laminated bag and stored at $-20\text{ }^{\circ}\text{C}$ until further analysis.

Preparation of ginseng IDF powders

The ginseng IDF was milled coarsely using a disc-mill (FZ102, Taisite Instrument Co., Ltd., Tianjin, China), and then the powders were passed through 20–60 mesh, 60–80 mesh and 100–160 mesh sieves, such that three different particle size ginseng IDF were obtained. The superfine powders passed through mesh sized less than 400 mesh was prepared using a superfine mill (HMB-700S, Hongquan Machinery Co., LTD, Taiwan) by regulating the grinding time. The particle size of samples between 20 and 60 mesh, 60 and 80 mesh, 100 and 160 mesh and less than 400 mesh were designated as M20, M60, M100 and M400, respectively. All samples were sealed in aluminum-laminated bags and stored at $-20\text{ }^{\circ}\text{C}$ until use.

Particle size and microstructure measurement of ginseng IDF

Particle size distributions of the ginseng IDF powders were analyzed using a Mastersizer 3000 laser diffraction instrument (Malvern Instruments Ltd., Malvern, UK). The powder was dispersed in methanol prior to measurements. Dv 50 is considered the median particle diameter, which is the equivalent volume diameter at 50% cumulative volume. Correspondingly, Dv 10 and Dv 90 denote the volume diameter at 10 and 90% cumulative volume, respectively. Powder morphology was observed using an environmental scanning electron microscopy (ESEM; Quanta 250 FEG, FEI Company, USA) at 15 kV. Powders were coated with gold, attached to a double-sided adhesive tape, and observed at $200\times$ magnification.

Hydration properties

WHC and water solubility index (WSI) were determined according to a method reported by Phat et al. [17]. For WHC quantification, 0.5 g (H) of sample was added to 10 mL of distilled water and mixed in a 15 mL centrifuge tube (W1). Afterwards, the reaction mixture was subjected to incubation in a water bath (DK500, Jing Hong Laboratory Instrument Co., Ltd., Shanghai, China) at $60\text{ }^{\circ}\text{C}$ for 30 min and subsequently centrifuged at 3000 rpm for 15 min (TD5A-WS, Xianglu Centrifuge Apparatus Co., Ltd., Changsha, China). The sediment tubes were then weighed (W2) and WHC was calculated based on the formula:

$$\text{WHC (g/g)} = (W_2 - W_1)/H \quad (1)$$

For WSI quantification, About 10 mL of distilled water was mixed with 0.2 g of powder in a tube, which was placed in a water bath at $80\text{ }^{\circ}\text{C}$ for 30 min. After

centrifugation at 3000 rpm for 10 min, the supernatant was transferred to a pre-weighed dish (S1) and dried at $105\text{ }^{\circ}\text{C}$ to constant weight (S2). WSI was calculated using the formula:

$$\text{WSI (\%)} = (S2 - S1)/S \quad (2)$$

Color values

Ginseng IDF samples of color properties (L^* , a^* and b^* values) were measured by colorimeter (CM-3600A, Konica Minolta, Osaka, Japan). The sample (powder) was placed on a glass plane and the colorimeter was placed directly on to the sample to measure the color values. The calibration of the equipment was performed by a white tile prior to recording sample color values and standard values were these: $L^*=86.90$, $a^*=0.3170$, and $b^*=0.3240$.

Bulk density, tap density, flowability, and cohesiveness

The bulk and tapped densities were measured according to the method described by Ramachandriah and Chin [18]. The flowability and cohesiveness of the samples were evaluated by the Carr index (%) [19] and Hausner ratio [20], respectively. The Carr index and Hausner ratio were calculated as shown below;

$$\text{Carr index (\%)} = (\text{Tap density} - \text{Bulk density}) / \text{Tap density} \times 100 \quad (3)$$

$$\text{Hausner ratio} = \text{Tap density} / \text{Bulk density} \quad (4)$$

Samples with Carr index values $<15\%$ very good, $15\text{--}20\%$ were considered good, $20\text{--}35\%$ fair, $35\text{--}45\%$ bad, and very bad if $>45\%$ [21]. Hausner ratio values <1.2 were considered to have low cohesiveness, Hausner ratio values 1.2 to 1.4 were intermediate, and the Hausner ratio value >1.4 were considered to have high cohesiveness [21].

Mineral content

Each ginseng IDF (0.5 g) was added with 10 mL deionized water and boiled for 15 min. Each sample was then centrifuged at 3500 rpm for 10 min and filtered using Whatman filter paper no. W1. After that, liquid solution (1 mL) was transferred to a 50 mL volumetric flask with deionized water and analyzed. An atom absorption spectrophotometer (AFS-8230, Titan Instruments Co., Ltd, Beijing, China) was used to determine the elemental composition (K, Ca, Na, Mg, Zn, Fe, Mn and Cu) in ginseng IDF samples.

Preparation of phenolic extracts

The ginseng IDF samples were extracted according to a method by Jiang et al. [22]. The samples (2 g) were homogenized with 20 mL methanol (80%) for 5 min and then extracted by sonication for 20 min. Homogenization and sonication treatments were performed repeatedly followed by filtration with a No 1. filter paper (Whatman Ltd., Cambridge, UK). The supernatant of each sample was collected, concentrated in vacuum, and stored at $-20\text{ }^{\circ}\text{C}$ before being analyzed.

Total phenolic content (TPC)

TPC was determined for each sample based on the method described by Eghdami and Sadeghi [23]. Diluted extract (200 μL) was added to Folin-Ciocalteu reagent (800 μL) and 7.5% sodium carbonate (2 mL). Distilled water used to dilute the mixture before being incubated at room temperature under dark condition for 2 h. The absorbance values were measured at 765 nm using a UV spectrophotometer (UV-1800, Shimadzu Instruments Mfg. Co., Ltd, Kyoto, Japan). The TPC was expressed as gallic acid equivalents (mg GAE 100 g^{-1}) on dry weight (DW) basis.

1,1-Diphenyl-2-picrylhydrazyl radical-scavenging activity (DPPH-RSA)

The DPPH-RSA of the samples was determined using the method described by Kang et al. [24]. Methanolic extract (50 μL) was added to 80% methanol (50 μL), and mixed with 0.2 mM DPPH radical solution (2 mL). The vortexed mixture (30 s) and stored at $25\text{ }^{\circ}\text{C}$ for 30 min. Sample absorbance of the mixture was measured at 517 nm using a spectrophotometer.

Reducing power (RP)

RP was determined as described by Huang et al. [25]. Methanolic extract (0.3 mL) was added with 1.1 mL phosphate buffer (0.2 M, pH 6.6) and mixed. To this mixture, 0.6 mL of 1% potassium ferricyanide was added and incubated at $50\text{ }^{\circ}\text{C}$ for 20 min. Following incubation, 10% trichloroacetic acid (1 mL) was added and centrifuged at $2016\times g$ for 15 min. The supernatant was separated and mixed with distilled water (1 mL) and 0.1% ferric chloride (0.5 mL). Sample absorbance was measured at 700 nm; increased absorbance corresponded to higher RP.

Hemolysis of mice erythrocytes

The maintenance of mice was carried out using a laboratory diet and water ad libitum until they were 6 weeks old. Experimental female mice weighing 18–20 g were fed in an environment of temperature $20\text{--}24\text{ }^{\circ}\text{C}$, humidity 50–70%, and 12 h alternate light and dark. All of the animal procedures were conducted in adherence to the

animal welfare guidelines and ethical committee compliance. Whole blood collected from experimental mice was added with anticoagulant heparin sodium and then centrifuged at 5000 rpm for 10 min. The plasma was discarded, and the erythrocytes isolated were washed with cold phosphate-buffered saline three times. Each phenolic extract (0.3 mL) from the different particle sizes (M20, M60, M100 and M400) was added with 0.1 mL mice erythrocytes suspension (0.5%), followed by the addition of 0.1 mL of 100 mmol/L H_2O_2 . The test tubes were incubated at $37\text{ }^{\circ}\text{C}$ for 1 h, and then added with 5.2 mL normal saline [26]. The samples were then centrifuged at 4000 rpm for 10 min, and the absorbance measured at 415 nm (Optizen 2120 UV; Mecasys Co., Daejeon, Korea).

Differential scanning calorimetry

Ginseng IDF powder samples (10–20 mg) were weighted accurately, sealed in aluminum pans and analyzed using DSC (Cph60, Netzsch, Germany). Temperature scans were conducted from 20 to $200\text{ }^{\circ}\text{C}$ at a heating rate of $10\text{ }^{\circ}\text{C}/\text{min}$. Each sample was measured at least in triplicate. The Universal Analysis 2000 software (TA Instruments Co., New Castle, USA) was applied to analyze the curve of each sample.

Fourier-transform infrared (FT-IR) spectroscopy

The organic functional groups of ginseng IDF samples were analyzed using a FT-IR spectrophotometer (FTIR/NIR 400, Perkin-Elmer Inc., Waltham, MA, USA). The spectrum wavelength was $400\text{--}4000\text{ cm}^{-1}$ at 4 cm^{-1} resolution with 4 scans at a scan speed of $<10\text{ s}$.

Statistical analysis

All analyses were performed in triplicate and values were presented as mean \pm standard deviation. One-way analysis of variance (ANOVA) was used to determine differences between treatments and were carried out in SPSS version 18.0 (Chicago, IL, USA). The differences in means were evaluated using the Duncan's multiple-range tests for means with 95% confidence limit ($p \leq 0.05$).

Results and discussion

Particle size reduction

It is known that the reduction in particle size and increased surface area could influence several powder properties. Particle sizes of ginseng IDF as affected by disc mill and superfine grinding are shown in Table 1. Although the difference in the average particle size of M20 and M60 was large, the specific surface was not ($p > 0.05$) affected. However, when ginseng IDF was subjected to vibrating superfine mill treatment, powder with highly ($p \leq 0.05$) reduced particle size and increased

specific surface area was formed. This is because vibrating superfine mill treatment caused greater breakage of the physical structure than disc mill. Similar reduction in particle size was observed in a study by Wen et al. [12], wherein rice bran dietary fibers were modified using enzyme-ball mill treatments. In another study, superfine powder was formed when rice bran IDF were milled in a vibrating superfine mill [15]. However, the span values, which indicate the width of the particle size distribution was increased upon superfine grinding. Similar increases in span values were also observed in rice bran IDF [15]. On the other hand, decreased span values were observed in *Lentinus edodes* mushroom powder [14]. Apart from the nature of the materials, the milling method and time also influence span values. It is important to note that micronization is a dynamic process that encompasses physical forces of fracture, breakage, and aggregation [27].

ESEM

Changes in the microstructure of ginseng IDF powders are illustrated in Fig. 1. As shown in Table 1, the particle size of M20, M60, and M100 are considerably larger than M400. Superfine powders (M400) show smaller particles of varying sizes as opposed to large blocky particles in the other three powders. Smaller particles that seem to have broken off from larger particles indicate the impact of superfine grinding on ginseng IDF. Large particles of ginseng IDF with porous surface was also shown in another study [5]. The lack of smooth surface is attributed to the loss of water soluble components during processing [3].

Hydration properties and color values of ginseng IDF powders

Hydration properties of ginseng IDF powders with different particle sizes are shown in Table 2. Although disc milling of ginseng IDF reduced the particle size, it had no

Table 1 Particle size distribution of ginseng IDF powders

	Dv (10) (μm)	Dv (50) (μm)	Dv (90) (μm)	Specific surface area (m ² /kg)	Span
M20	812.00 ± 12.29a	1443.33 ± 25.17a	2496.672 ± 0.82a	10.40 ± 0.96a	0.69 ± 0.01c
M60	624.00 ± 3.46b	880.33 ± 11.68b	1216.67 ± 35.12b	10.48 ± 0.29a	0.67 ± 0.03c
M100	110.67 ± 0.58c	182.67 ± 0.58c	273.00 ± 1.00c	69.15 ± 2.01b	0.90 ± 0.02b
M400	3.74 ± 0.01d	15.83 ± 0.29d	33.63 ± 0.21d	750.30 ± 1.25c	1.87 ± 0.01a

Values represent means ± standard deviations; Means followed by different letters (a–d) in the same column represent statistically significant differences (p ≤ 0.05)

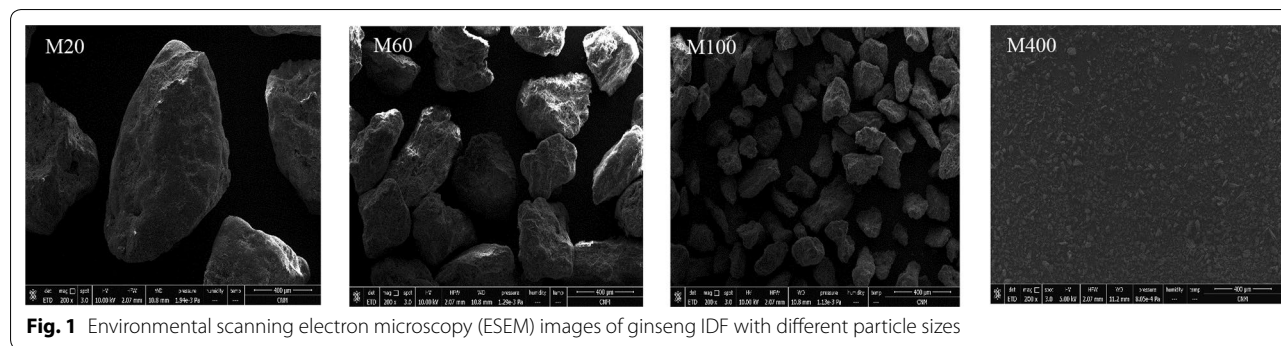


Fig. 1 Environmental scanning electron microscopy (ESEM) images of ginseng IDF with different particle sizes

Table 2 Hydration properties and color values of ginseng IDF as affected by different particle sizes

	WHC (g g ⁻¹)	WSI (%)	Color values		
			L*	a*	b*
M20	3.88 ± 0.08b	6.08 ± 0.32b	55.39 ± 0.28c	5.61 ± 0.06a	7.80 ± 0.06d
M60	4.09 ± 0.18b	6.95 ± 0.86b	54.96 ± 0.17c	4.27 ± 0.04b	10.08 ± 0.05c
M100	3.97 ± 0.18b	7.73 ± 1.03b	61.39 ± 0.14b	3.57 ± 0.10c	12.95 ± 0.30b
M400	5.15 ± 0.42a	13.38 ± 1.31a	75.81 ± 0.22a	2.73 ± 0.02d	17.49 ± 0.53a

WHC: water holding capacity; WSI: water solubility index

Values represent means ± standard deviations; Means followed by different letters (a–d) in the same column represent statistically significant differences (p ≤ 0.05)

impact on WHC. However, superfine grinding resulted in increased WHC. Increased WHC of superfine powders was also seen with rice bran IDF [13]. Likewise, WSI increased significantly only for superfine powders. Improved hydration properties of superfine powders are due to increased surface area, which causes higher exposure of polar groups to water. Increased polar groups present as binding sites for water. Studies have indicated the increased porosity of particles could also affect its ability to hold water via hydrogen bonding [15]. Particle size reduction resulting in increased solubility was also seen in other study with *Hericium erinaceum* powders [17]. Increased solubility has been attributed to shorter cellulose chains and higher exposure of hydrophilic cellulose and hemicellulose groups as a result of superfine grinding [28]. When products such as instant food are developed, the hydration property, WSI, is a major consideration.

The color values of ginseng IDF powders as affected by different particle sizes are given in Table 2. The L^* (lightness) and b^* (yellowness) values of powders showed significant ($p \leq 0.05$) increases with corresponding rises in powder mesh sizes from M20 to M400. It was found that reduction of particle size conferred more degree of brightness to powder product. On the other hand, the a^* (redness/greenness) values showed significant decreases with increases in mesh sizes. This implied that superfine grinding led to decreasing tendency of redness in powdered products. The increases in degree of yellowness might be attributed to the aggregation phenomenon of phenolic compounds after exposure to superfine grinding. These results are in correspondence with the findings of previously reported study in which decreases in particle sizes led to increases in lightness and yellowness during superfine grinding of celery stalk powders [18].

Bulk and tapped densities, and flowability

Bulk and tapped densities as well as flowability are also shown in Table 3. Decreasing particle sizes resulted in decreasing bulk and tapped density. This is contrary to other studies wherein particle size reduction caused increased bulk density [17]. However, decreased bulk and tapped density indicates open packed structures of

powders subjected to superfine grinding. Studies show that bulk density is associated with particle size distributions, surface weighted mean $D(3, 2)$, and fineness. Lower surface weighted mean is associated with higher cohesiveness [29]. However, in this study, $D(3, 2)$ values of M20, M60, M100 and M400 were $583.3 \pm 4.6 \mu\text{m}$, $555.0 \pm 4.3 \mu\text{m}$, $87.2 \pm 2.7 \mu\text{m}$ and $8.0 \pm 0.02 \mu\text{m}$, respectively. As shown in Table 3, reduced particle sizes resulted in increased cohesiveness of ginseng IDF powders. This is based on the Hausner ratio, which increased with reduced particle size indicating higher cohesiveness. Nonetheless, particles within cohesive superfine powders tend to aggregate and form larger particles that are held together by inter-particle forces. Cases in which external force is unable to break such inter-particle forces between larger particles can cause loose packing of powders, which in turn decreases the bulk density [30]. Bulk and tap densities are considered in the development of aqueous food products, such as instant beverages or soup mixes [17]. However, in this study, lower particle size increased the Carr values, which in turn lowered the flowability of ginseng powders from very good to fair to poor. Carr index values should be considered when powders are poured, sieved, and mixed during processing [31].

Mineral element, TPC and antioxidant activities

The results of mineral content analysis for ginseng IDF with different particle are shown in Table 4. Ginseng residue insoluble dietary fibers have been shown to contain mineral elements such as calcium, sodium, magnesium, potassium, copper, manganese, and zinc etc. [3]. Mineral and inorganic components are essential for several purposes and play a vital role in metabolism [32]. However, in this study, the mineral elements detected were calcium, potassium, magnesium, manganese, zinc, copper and iron. Powders with the largest particle size contained Ca, K and Mg. However, as the particle size reduced, the mineral content of Ca, K and Mg were increased. The particles with the smallest size was found to contain Mn, Zn and Fe. These results indicate that particle size reduction caused higher extraction of mineral content.

Table 3 Density, flowability, and cohesiveness of ginseng IDF as affected by different particle sizes

	Bulk density (g/cm ³)	Tapped density (g/cm ³)	Carr index (%)	Flowability	Hausner ratio	Cohesiveness
M20	0.77 ± 0.01a	0.82 ± 0.03a	5.49 ± 3.04c	Very good	1.06 ± 0.03c	Low
M60	0.69 ± 0.02b	0.75 ± 0.01b	7.68 ± 2.52c	Very good	1.08 ± 0.03c	Low
M100	0.64 ± 0.01c	0.76 ± 0.02b	16.56 ± 0.89b	Good	1.20 ± 0.01b	Intermediate
M400	0.28 ± 0.02d	0.48 ± 0.02c	42.25 ± 2.32a	Bad	1.730 ± .07a	High

Values represent means ± standard deviations; Means followed by different letters (a–d) in the same column represent statistically significant differences ($p \leq 0.05$); Carr index (which indicates flowability): very good (< 15%), good (15–20%), fair (20–35%), bad (35–45%), very bad (> 45%); Hausner ratio value: low cohesiveness (< 1.2), intermediate cohesiveness (1.2–1.4), high cohesiveness (> 1.4) [19]

Table 4 Mineral content of ginseng IDF with different particle sizes (Unit: $\mu\text{g/g}$)

	Ca	K	Mg	Mn	Zn	Cu	Fe
M20	0.437 \pm 0.016c	4.840 \pm 0.004d	0.664 \pm 0.004d	–	–	–	–
M60	0.542 \pm 0.015b	5.201 \pm 0.006c	0.681 \pm 0.003c	–	–	–	–
M100	0.547 \pm 0.008b	5.435 \pm 0.006b	0.716 \pm 0.001b	–	–	–	0.027 \pm 0.010
M400	0.910 \pm 0.007a	8.511 \pm 0.007a	1.137 \pm 0.001a	0.020 \pm 0.001	0.021 \pm 0.015	–	0.041 \pm 0.030

– Not detected

Values represent means \pm standard deviations; Means followed by different letters (a–d) in the same column represent statistically significant differences ($p \leq 0.05$)

Effect of particle size on TPC is shown in Fig. 2a. Decreasing particle size resulted in increasing TPC. Particles of superfine ginseng powders had the highest TPC. Increased TPC due to superfine grinding has also been reported in other studies on wine grape pomace [33] and rice bran IDF [15]. Ginseng has been reported to contain a variety of phenolic compounds. In a study, 23 different types of phenolic compounds were identified. Particularly, gentisic acid, rutin, p- and m-coumaric acid, and chlorogenic acid were reported to be the main phenolic compounds present in *Panax ginseng* [34]. In a previous investigation, 12 different free, esterified, and insoluble-bound forms of phenolic acids were identified. The predominant free phenolic acid was *trans*-Ferulic acid, esterified phenolic acids were *cis*-ferulic acid and *trans*-ferulic acid and the main insoluble-bound phenolic acid was Ferulic acid (*cis* and *trans* isomers) [35]. However, in this study, smaller particles due to increased surface and improved extraction caused an increase in TPC. DPPH-RSA, which relates to the antioxidant activity of ginseng IDF is shown in Fig. 2. Similar to the trend of TPC values, DPPH-RSA also increased with decreasing particle size. DPPH-RSA for M20, M60, M100 and M400 was 13.29%, 23.88%, 25.54% and 39.21%, respectively. The smallest particle size IDF exhibited the highest RSA. Elevated levels of RSA could be directly associated with increased TPC. These results are consistent with another study on rice bran IDF [15]. However, higher DPPH-RSA is not always related to increased TPC. Despite the decrement in particle size, DPPH RSA was not increased, as seen in other studies [33]. Likewise, RP assay is also employed to measure the antioxidant activities of ginseng IDF. RP, as shown in Fig. 2, was also consistent with the TPC. Ginseng IDF with the largest particle size had the lowest activity. When compared with M20, reducing power increased by 28.8%, 36.6% and 90% for M60, M100 and M400, respectively. The antioxidant potential of ginseng has been demonstrated in a clinical study, wherein level of serum ROS and methane dicarboxylic aldehyde activity were reduced in healthy volunteers [36]. However, in this study, with decrement in particle size, increases in surface area could have caused greater exposure and release of phenolic contents from fibrous matrix, which

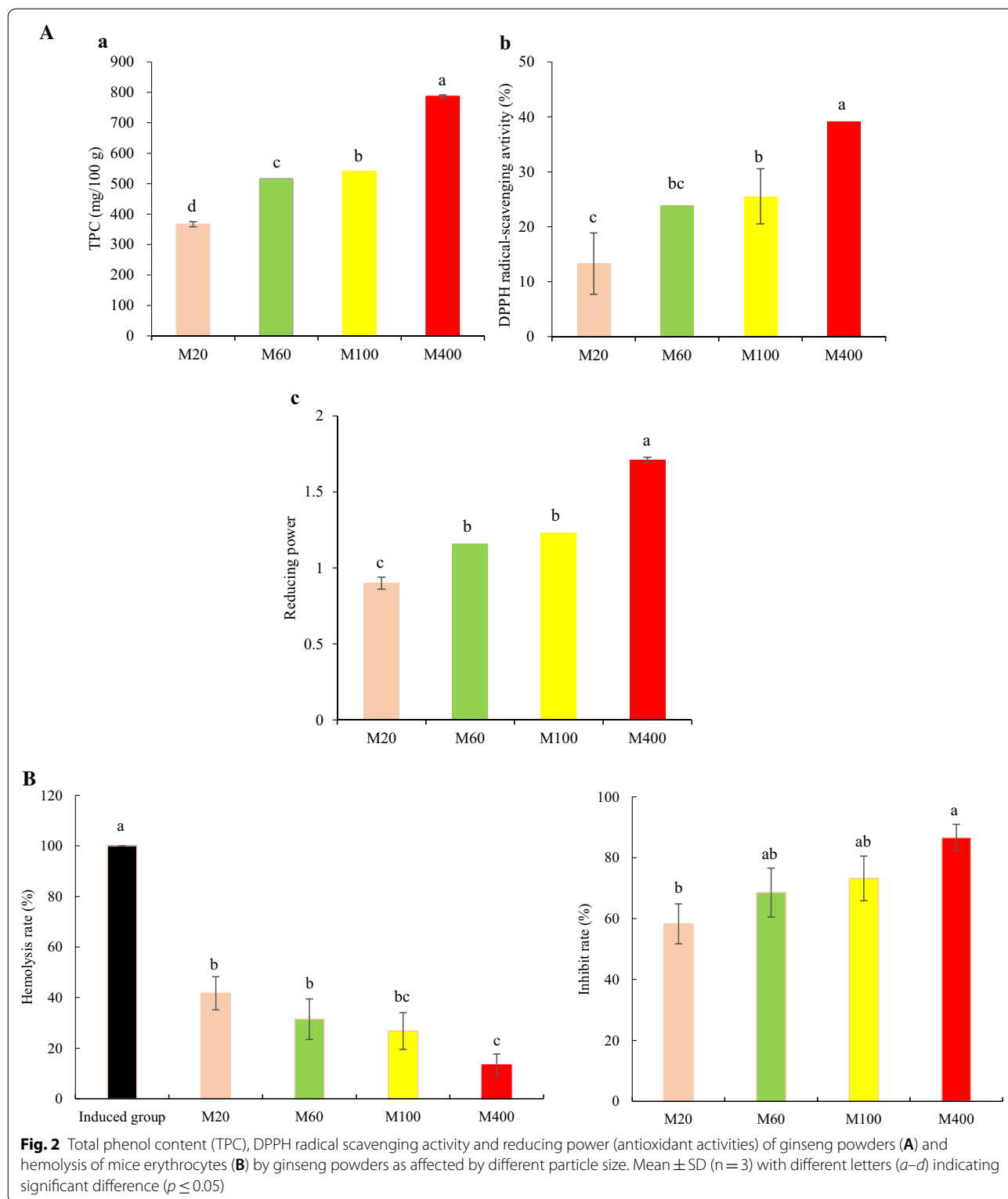
in turn could have improved antioxidant activity. Since several traditional materials have been adopted as modern medicines, it is likely that ginseng powders can also be utilized in the development of new therapeutic agents [37].

Hemolysis of mice erythrocytes

It is known that oxidative damage by reactive oxygen species occurs through the peroxidation of erythrocyte membranes. Oxidative damage induced by H_2O_2 can elevate erythrocyte hemolysis and the inhibition rate [26]. In this study, RBC hemolysis percentage decreased with decreasing particle size (Fig. 2b). Contrarily, hemolysis inhibition rate increased with decreasing particle size. This is likely due to the increased extraction of polyphenols with the decreasing particle size of ginseng powders. Studies have shown that polyphenols binding to RBC membrane matrix, particularly to tryptophan residues, can inhibit oxidation of lipids and induce antihemolytic activity [38]. In this study, the smallest particle size (M400) had the highest erythrocyte hemolysis inhibition rate of 86.6%, which was higher than other ginseng IDFs. As shown in Fig. 2a, increased TPC with decreasing ginseng particle size could have contributed to such inhibition rates. A similar effect of the concentration of polyphenols from mulberry fruit on the hemolysis rate and inhibition rate of red blood cells from mice induced by H_2O_2 was observed in another study. Increasing polyphenol concentration decreased the mice erythrocytes hemolysis rate and increased the inhibition rate [26].

Thermal analysis of ginseng IDF

The transition temperature (T_{p1}) and melting peak temperatures (T_{p2}) of ginseng IDF with different particle sizes in shown in Table 5. The transition temperature (T_{p1}) tended to reduce with decreasing particle size. The smallest particle size powder (M400) had the lowest T_{p1} . Endothermic peaks (T_{p2}) for all the samples were observed to be between 80 and 125 °C. The peak temperatures also decreased with decreasing particle size. Similar results were observed for sugar beet pulp powders [39]. These results are in contrast with another study on white winter wheat bran, wherein decreasing particle



size resulted in a decreasing tendency for peak temperatures [40]. In this study, it is likely that the reducing particle size could have caused greater exposure of

polysaccharide and protein groups, thereby lowering the peak temperatures.

Table 5 The transition temperature (Tp1) and melting peak temperatures (Tp2) of ginseng IDF as affected by different particle sizes

	Tp1 (°C)	Tp2 (°C)
M20	46.07 ± 1.53a	120.50 ± 4.53a
M60	42.20 ± 2.96ab	110.60 ± 1.22b
M100	37.77 ± 5.56bc	88.10 ± 3.44c
M400	31.60 ± 4.43c	80.70 ± 3.32d

Values represent means ± standard deviations; Means followed by different letters (a–d) in the same column represent statistically significant differences ($p \leq 0.05$)

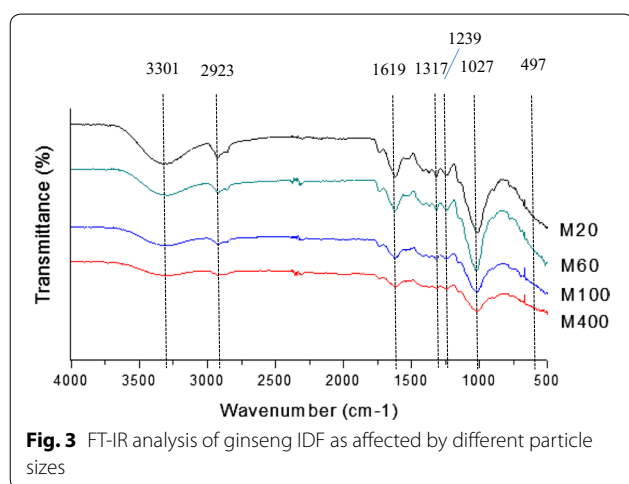


Fig. 3 FT-IR analysis of ginseng IDF as affected by different particle sizes

FT-IR analysis of ginseng IDF

FT-IR spectra of ginseng IDF with different particle sizes are shown in Fig. 3. Functional groups such as OH, NH, and CO can be qualitatively evaluated via FT-IR analysis [41]. The OH group stretching at 3300–3500 is associated with phenolic structures [41]. In this study, the peaks formed at 3301 cm^{-1} correspond to –OH stretch vibration, which indicates the presence of phenolic structures. The FT-IR spectra in this study was similar to that of ginseng IDF [5]. However, the decrease in intensity in this region of spectra for different powders could be attributed to the breakdown of intermolecular bonds due to the physical force of milling [42]. Similar bands formed at these frequency ranges were also observed in another study [43]. The major absorption peak at 2923 cm^{-1} is due to the C–H stretching indicating the presence of cellulose [42, 44]. Similarly, in an earlier study, peak at 2924 cm^{-1} was assigned to C–H stretching of grape pomace powders [13]. The major peak at 1619 cm^{-1} can be attributed to the esterified and ionized carboxyl groups of galacturonic acid [3]. The peak corresponding to CH bonds indicate the presence the aromatic molecules as also shown in another study [13, 43]. The weak

peaks at 1317 cm^{-1} and 1239 cm^{-1} can be ascribed to the cellulose and hemicellulose structures, respectively. The peaks formed around 1027 cm^{-1} for ginseng IDF with different particle size distributions indicated stretching vibration of C–O [43]. Furthermore, the decrease in absorbance intensity of peaks is associated with the changes in the surface properties of the finer powders. Similar decrement in the intensity associated with lower particle size was also observed in a recent study on *Moringa Oleifera* leaf powders [45]. The lack of disappearance of the major phenolic compounds in the profiles of different ginseng powders suggested that the particle size reduction did not affect the major structure of phenolics.

Acknowledgements

This study was financially supported by Jilin Medical University (Project Number: JYBS2019010), Jilin Province, China.

Authors' contributions

Project administration & experiment & writing, GJ; Writing & experiment, SL; Experiment, ZW; Analysis, KA; Writing—review & editing, KR. All authors read and approved the final manuscript.

Funding

This study was financially supported by Jilin Medical University, Jilin Province, China (Project Number JYBS2019010).

Availability of data and materials

The datasets used and/or analyzed during the current study are available from the first and corresponding author on reasonable request.

Competing interests

The authors report no conflicts of interest.

Author details

¹ School of Public Health, Jilin Medical University, Jilin 132013, China. ² Department of Food Science and Biotechnology, Sejong University, Seoul 05006, South Korea. ³ Department of Food Science and Technology, Graduate School of Chonnam National University, Gwangju 61186, Republic of Korea.

Received: 8 August 2020 Accepted: 24 October 2020

Published online: 04 November 2020

References

- Kendall CWC, Esfahani A, Jenkins DJA (2010) The link between dietary fiber and human health. *Food Hydrocolloid* 24:42–44
- Makki K, Deehan EC, Walter J, Backhed F (2018) The impact of dietary fiber on gut microbiota in host health and disease. *Cell Host Microbe* 23:705–715
- Stephen AM, Champ MM, Cloran SJ, Fleith M, Lieshout L, Mejbourn H, Burley VJ (2017) Dietary fiber in Europe: current state of knowledge on definitions, sources, recommendations, intakes and relationships to health. *Nutr Res Rev* 30:149–190
- Alba K, MacNaughtan W, Laws AP, Foster TJ, Campbell GM, Kontogiorgos V (2018) Fractionation and characterisation of dietary fiber from blackcurrant pomace. *Food Hydrocolloid* 81:398–408
- Hua M, Lu JX, Qua D, Liu C, Zhang L, Li SS, Chen JB, Sun YS (2019) Structure, physicochemical properties and adsorption function of insoluble dietary fiber from ginseng residue: a potential functional ingredient. *Food Chem* 286:522–529
- Carlson JL, Erickson JM, Lloyd BB, Slavin JL (2018) Health effects and sources of prebiotic dietary fiber. *Curr Dev Nutr* 2(3):nz005

7. Zhang Y, Zhang Y, Taha AA, Ying Y, Li X, Chen X et al (2018) Subcritical water extraction of bioactive components from ginseng roots (*Panax ginseng* C.A. Mey). *Ind Crop Prod* 117:118–127
8. Park SY, Lee KY, Cho YJ, Park BK, Kim KJ, Lee NR, Kim YH, Hahn TW (2015) Efficacy of orally administered ginseng stem and leaf in chickens. *Korean J Vet Res* 55(1):1–7
9. Shergis JL, Di YM, Zhang AL, Vlahos R, Helliwell R, Ye JM, Xue CC (2014) Therapeutic potential of *Panax* ginseng and ginsenosides in the treatment of chronic obstructive pulmonary disease. *Complement Ther Med* 22:944–953
10. Iqbal H, Rhee DK (2019) Ginseng alleviates microbial infections of the respiratory tract: a review. *J Ginseng Res*. 44(2):194–204
11. Rivera E, Daggfeldt A, Hu S (2003) Ginseng extract in aluminium hydroxide adjuvanted Vaccines improves the antibody response of pigs to porcine parvovirus and *Erysipelothrix rhusiopathiae*. *Vet Immunol Immunop* 91:19–27
12. Wen Y, Niu M, Zhang B, Zhao S, Xiong S (2017) Structural characteristics and functional properties of rice bran dietary fiber modified by enzymatic and enzyme-micronization treatments. *LWT-Food Sci Technol* 75:344–351
13. Zhao X, Zhu H, Zhang G, Tang W (2015) Effect of superfine grinding on the physicochemical Properties and antioxidant activity of red grape pomace powders. *Powder Technol* 286:838–844
14. Ming J, Chen L, Hong H, Li JL (2014) Effect of superfine grinding on the physico-chemical, morphological and thermogravimetric properties of *Lentinus edodes* mushroom powders. *J Sci Food Agr* 95:2431–2437
15. Zhao G, Zhang R, Dong L, Huang F, Tang X, Wei Z, Zhang M (2018) Particle size of insoluble dietary fiber from rice bran affects its phenolic profile, bioaccessibility and functional properties. *LWT-Food Sci Technol* 87:450–456
16. Bunzel M, Ralph J, Kim H, Lu F, Ralph SA, Marita JM (2003) Sinapate dehydridimers and sinapate-ferulate heterodimers in cereal dietary fiber. *J Agr Food Chem* 51:1427–1434
17. Phat C, Li H, Lee DU, Moon BK, Yoo YB, Lee C (2015) Characterization of *Hericium Erinaceum* powders prepared by conventional roll milling and jet milling. *J Food Eng* 145:19–24
18. Ramachandiraiah K, Chin KB (2017) Impact of drying and micronization on the Physicochemical properties and antioxidant activities of celery stalk. *J Sci Food Agr* 97:4539–4547
19. Carr RL (1965) Evaluating flow properties of solids. *Chem Eng J* 72:163–168
20. Hausner HH (1967) Friction conditions in a mass of metal powder. *Int J Powder Metall* 3:7–13
21. Jinapong N, Suphantharika M, Jamnong P (2008) Production of instant soymilk powders by ultrafiltration, spray drying and fluidized bed agglomeration. *J Food Eng* 84:194–205
22. Jiang GH, Nam SH, Eun JB (2018) Effects of peeling, drying temperature, and sodium metabisulfite treatment on physicochemical characteristics and antioxidant activities of Asian pear powders. *J Food Process Preserv* 42:e13526
23. Eghdami A, Sadeghi F (2010) Determination of total phenolic and flavonoid contents in methanolic and aqueous extract of *Achillea Millefolium*. *J Org Chem* 2:81–84
24. Kang MH, Park CG, Cha MS, Seong NS, Chung HK, Lee JB (2001) Component characteristics of each extract prepared by different extract methods from byproducts of *Glycyrrhiza Uralensis*. *J Kor Soc Food Sci Nutr* 30:138–142
25. Huang SJ, Tsai SY, Mau JL (2006) Antioxidant properties of methanolic extracts from *Agracybe cylindracea*. *LWT-Food Sci Technol* 39:378–386
26. Ajay Krishna PG, Sivakumar TR, Jin C, Li SH, Weng YJ, Yin J, Jia JQ, Wang CY, Gui ZZ (2018) Antioxidant and hemolysis protective effects of polyphenol-rich extract from mulberry fruits. *Pharmacogn Mag* 14:103–109
27. Zhang LX, Xu HD, Li SF (2009) Effects of micronization on properties of *Chaenomeles sinensis* (Thouin) Koehne fruit powder. *Innov Food Sci Emerg Technol* 10:633–637
28. Hong J, Zhang SY (2005) Effect of ultra-fine pulverization by wet processing on particle structure and physical properties of soybean dietary fiber. *J South China Agr Uni* 10:90–94
29. Saw HY, Davies CE, Jones JR, Paterson AHJ (2014) Shear testing of lactose powders: the influence of consolidation stress and particle size on bulk density and estimated cohesion, Conference paper. *Adv Powder Technol* 25:1164–1170
30. Rajkhowa R, Kafi A, Zhou QT, Kondor A, Morton DAV, Wang X (2015) Relationship between processing, surface energy and bulk properties of ultra-fine silk particles. *Powder Technol* 270:112–120
31. Muttakin S, Kima MS, Lee DU (2015) Tailoring physicochemical and sensorial properties of defatted soybean flour using jet-milling technology. *Food Chem* 187:106–111
32. Adams S, Sello CT, Qin GX, Che D, Han R (2018) Does dietary fiber affect the levels of Nutritional components after feed formulation. *Fibers* 6:29
33. Zhu FM, Du B, Li J (2012) Effect of ultrafine grinding on physicochemical and antioxidant Properties of dietary fiber from wine grape pomace. *Food Sci Technol Int* 20:55–62
34. Chung IM, Lim JJ, Ahn MS, Jeong HN, An TJ, Kim SH (2016) Comparative phenolic compound profiles and antioxidative activity of the fruit, leaves, and roots of Korean ginseng (*Panax ginseng* Meyer) according to cultivation years. *J Ginseng Res* 40(1):68–75
35. Jung MY, Jeon BS, Bock JY (2002) Free, esterified, and insoluble-bound phenolic acids in white and red Korean ginsengs (*Panax ginseng* CA Meyer). *Food Chem* 79(1):105–111
36. Yang Y, Ren C, Zhang Y, Wu X (2017) Ginseng: a nonnegligible natural remedy for healthy aging. *Aging Dis* 8(6):708–720
37. Ratan ZA, Haidere MF, Hong YH, Park SH, Lee JO, Lee J, Cho JY (2020). Pharmacological potential of ginseng and its major component ginsenosides. *J Ginseng Res* In press
38. Loganayaki N, Siddhuraju P, Manian S (2013) Antioxidant activity and free radical scavenging Capacity of Polyphenol extracts from *Helicteres isora* L. and *Ceiba pentandra* L. *Food Sci Technol* 50:687–695
39. Huang X, Dou JY, Li D, Wang LJ (2018) Effects of superfine grinding on properties of sugar beet pulp powders. *LWT-Food Sci Technol* 87:203–209
40. He S, Li J, He Q, Jian H, Zhang Y, Wang J, Sun H (2018) Physicochemical and antioxidant properties of hard white winter wheat (*Triticum aestivum* L.) bran superfine powder produced by eccentric vibratory milling. *Powder Technol* 325:126–133
41. Zhang ZF, Lv GY, He WQ, Shi L, Pan H, Fan L (2013) Effects of extraction methods on the antioxidant activities of polysaccharides obtained from *Flammulina velutipes*. *Carbohydr Polym* 98:1524–1531
42. Zhao X, Chen J, Chen F, Wang X, Zhu Q, Qiang A (2013) Surface characterization of corn stalk superfine powder studied by FTIR and XRD. *Colloid Surf B* 104:207–212
43. Fu C, Yang X, Lai S, Liu C, Huang S, Yang H (2015) Structure, antioxidant and α -amylase inhibitory activities of longan pericarp proanthocyanidins. *J Func Foods* 14:23–32
44. Baeza J, Freer J, Hon DNS, Shiraiishi N (2001) Chemical characterization of wood and its components: wood and Cellulosic Chemistry. Marcel Dekker, New York, p 275
45. Huang X, Liang K, Liu Q, Qiu J, Wang J, Zhu H (2020) Superfine grinding affects physicochemical, thermal and structural properties of *Moringa Oleifera* leaf powders. *Ind Crop Prod* 151:112472

Publisher's Note

Springer Nature remains neutral with regard to jurisdictional claims in published maps and institutional affiliations.